Accurate Prediction of Adiabatic Ionization Energies for PAHs and Substituted Analogues

Jérémy Bourgalais, Xavier Mercier, Muneerah Mogren Al-Mogren, Majdi Hochlaf

Accurate Prediction of Adiabatic Ionization Energies for PAHs and Substituted Analogues: *Advancements with the M06-2X Density Functional Theory Method*

Jérémy Bourgalais,[1,*] Xavier Mercier,[2] Muneerah Mogren Al-Mogren,[3] and Majdi Hochlaf [4,*]

ABSTRACT

Accurate calculation of AIEs for PAHs and their substituted analogues is important for understanding their electronic properties, reactivity, stability, and environmental/health implications. This work demonstrates that the M06-2X density functional theory (DFT) method performs well in predicting the adiabatic ionization energies (AIEs) of polycyclic aromatic hydrocarbons (PAHs) and related molecules, outperforming common DFT methods and competing in accuracy to the highly accurate CCSD(T)-F12 method. The accuracy of M06-2X is attributed to its large quantity of Hartree-Fock (HF) exchange and its ability to describe diffuse wave functions, which may make it suitable for predicting electronic properties associated with Rydberg-like electronic states. This suggests that M06-2X, with an appropriate basis set, is a reliable and efficient method for studying the PAHs and related molecules in conjunction with experimental techniques. The set of molecules used in this work includes also PAHs with hetero-atoms that can be found in biofuels or nucleic acid bases, making it of great interest for photoionization experiments and mass spectrometry. Down the road, this method will help understanding the relationship of various PAHs to graphene, guiding material research or electronic applications, and validating theoretical calculation methods.

Polycyclic aromatic hydrocarbons (PAHs) are a type of organic compound composed of fused aromatic rings. In PAHs, all carbon atoms are sp^2 hybridized, resulting in a highly stable and fully conjugated delocalized aromatic π-electron system, which allows for a planar structure, assuming there are no steric repulsions present. PAHs are produced during incomplete combustion of organic matter and can be found in various environmental sources such as air, food, water, and soil.[1–3] Due to their wide distribution and potential toxicity, PAHs and their formation mechanisms have been extensively investigated in fields such as atmospheric sciences,[4,5] astrochemistry,[6–8] combustion science,[9–13] and material sciences.[14,15]

The ionization energy is a fundamental electronic property that plays a pivotal role in comprehending the properties and behavior of PAHs, as well as other organic compounds and materials. Precise predictions of PAH ionization energies can yield valuable insights into their chemical reactivity, as these energies are directly correlated to molecular stability and reactivity. Knowledge of PAH ionization energies can guide the design of novel materials targeting desired electronic properties and aid in the interpretation of experimental data, such as spectroscopic measurements and chemical reactions involving PAHs. Moreover, the ionization energy is closely intertwined with the electronic structure of PAHs, as it reflects the distribution and energy levels of molecular orbitals, as well as the stability of charged species. Understanding the electronic structure of PAHs is crucial for predicting their optical properties, electronic transport properties, and environmental behavior. Accurate predictions of ionization energies serve as a foundation for elucidating the behavior of PAHs in various systems and applications, and facilitate the optimization of PAH-based materials for diverse technological and environmental purposes.

The ionization energy of PAHs can be investigated through a combination of experimental and theoretical approaches. Experimental methods such as photoionization mass spectrometry and photoelectron spectroscopy involve exposing molecules to soft photon sources, typically in the vacuum ultraviolet (VUV) range, which promotes electrons from the ground state of neutral species to higher-energy states of the ionized respective compounds. By analyzing the photon energy at which the first ionization event occurs and examining the resulting mass spectra for fragmentation patterns and relative abundances of the ionized fragments, the ionization energies, as well as the molecular structure and properties, can be estimated. Photoelectron spectra can also provide information about the kinetic energies of the ejected electrons, which can offer insights into the ionization energy and electronic structure of PAHs.[16–21]

Theoretical calculations using quantum chemistry methods also complement experimental measurements by providing estimates of the ionization energy of molecules. These methods involve solving the electronic Schrödinger equation for the molecule and obtaining the ionization energy from the energy difference between the neutral and ionized states. Historically, the “gold standard”

quantum method for determining ionization energies of monoconfigurational molecular systems has been the coupled cluster method with singles, doubles, and perturbative triples ((R)CCSD(T)) in conjunction with the aug-cc-pVTZ atomic basis set, which is known for its high accuracy and predictive potentialities.[22,23] However, (R)CCSD(T) has a computational cost that scales steeply with the size of the system as it involves calculating higher-order excitations and requires extensive memory and storage, making it impractical for studying large molecules such as PAHs. Instead, density functional theory (DFT)[24,25] is a popular alternative to coupled clusters methods due to its computational efficiency and relatively good accuracy for a wide range of systems. However, despite its widespread success, the use of approximate exchange-correlation functionals provide different levels of accuracy, depending on the specific system being studied and the properties of interest.[24,26] In DFT, the electron density is treated as the basic variable, and the electron-electron correlation effects are approximated through the exchange-correlation functional.

In recent years, advancements in DFT methods, such as hybrid functionals, have shown promise in improving the accuracy of ionization energy calculations. However, the choice of functional can significantly impact the accuracy of predictions, and it is important to carefully select an appropriate functional for a given molecular system (see for instance Semmeq et al.[27]).In particular, hybrid functionals combine local exchange-correlation functional of DFT with a fraction of the exact exchange energy calculated from Hartree-Fock (HF) theory. The amount of HF exchange used in hybrid functionals is analogous to the electronic correlation energy considered in CCSD(T) *ab initio* methods. Electron correlation effects can be significant in PAHs due to their large size and delocalized π-electron systems, leading to strong static and dynamic correlation effects to be accounted for. Among hybrid functionals, M06-2X[28] is known for its accuracy in predicting a wide range of molecular properties, including bond lengths, bond angles, reaction energies, and noncovalent interactions. For ionization energies, M06-2X has been identified as the most promising functional within the Minnesota family[29] and exhibiting strong competitiveness with other functionals.[30]

In this work, we present a significant breakthrough in computational chemistry by demonstrating that M06-2X DFT can accurately calculate the adiabatic ionization energies (AIEs) of PAHs and substituted analogues across a wide range of molecular systems, having masses from low molecular mass (<100 u) to relatively high atomic mass (400 u). This work also demonstrates that the performance of M06-2X is comparable, in this context, to the widely regarded high-level *ab initio* explicitly correlated method (R)CCSD(T)-F12, which is used as reference for quantum chemical calculations. Indeed, this approach in conjunction with a basis set of aug-ccp-V(X)Z quality allows predicting molecular properties as accurate as the standard coupled clusters approach extrapolated to the complete basis set (CBS) limit, whereas a strong reduction of computational cost (both CPU

time and disks occupancy) is observed.[19,31,32] At the end of this manuscript, by employing the M06-2X method, predictions of the AIEs of coronene-derivatives are given and compared to the referenced AIE of graphene.

Table 1. Experimental reference AIE of naphthalene compared to the calculated AIEs using DFT and coupled cluster approaches. For DFT computations, we described the atoms using the 6-311++G(d,p) basis set.

Methods	AIE (eV)
Exp.	8.144[33]
DFT	
M06-2X	8.144
B3LYP	7.867
ωb97X-D	7.953
B3PW91	7.912
PBE0	7.893
B97-2	7.804
CAM-B3LYP	7.974
TPSSh	7.759
X3LYP	7.828
Composite	
CBS-QB3	8.173
G4	8.143
Coupled-clusters	
(R)CCSD(T)/CBS	8.137
(R)CCSD(T)-F12/aug-cc-pVDZ	8.121

Naphthalene ($C_{10}H_8$, m/z 128 a.u.) with its two fused benzene rings has first been chosen as a benchmark system for validating theoretical models due to its well-defined and accurately determined experimental AIE value. Indeed, the AIE of naphthalene was experimentally determined to be 8.144 $\pm$ 0.0009 eV using a two-color multiphoton ionization technique.[33] Table 1 compares the reference AIE value of naphthalene to calculated values with some of the commonly used hybrid DFT

functionals in quantum chemistry and computational chemistry along with composite methods and coupled clusters calculations (see computational methods section for more details).

M06-2X in conjunction with the 6-311++G(d,p) Pople basis set[34] has by far the most accurate AIE value among the DFT methods with similar basis set size and is in an excellent agreement with the reference AIE value. M06-2X includes 54% of HF exchange, which is higher than the amount of HF exchange included in many other widely used hybrid DFT functionals, such as B3LYP[35,36] (20%), PBE0[37] (25%), ωB97X-D[38] (10%). The higher amount of HF exchange in M06-2X can explain the present accurate determination compared to other DFT methods for naphthalene.

Interestingly, the AIE with M06-2X/6-311++G(d,p) is also more accurate than the values calculated with the composite methods (CBS-QB3, G4, Table 1). Typically, composite methods use a separate approach for geometry optimization and energy calculations. They employ high-level methods for energy calculations, while geometry optimization is performed using lower-level methods to reduce computational costs. The specific functional used for geometry optimization in composite methods may vary depending on the composite method being used. Some commonly used methods, such as the Gaussian-n (Gn) series of methods like G4[39], employ HF or post-HF methods, such as MP2 or CCSD(T), for geometry optimizations. Other composite methods, such as the CBS-QB3[40,41] technique, use semiempirical methods, such as AM1 or PM3, for geometry optimizations. Semiempirical methods are approximate quantum mechanical methods that relay on simplified Hamiltonians and empirical parameters to describe molecular electronic structure. In G4, the geometry optimization is typically performed using a high-level *ab initio* method, that includes electron correlation effects beyond the mean-field approximation of the HF theory. This may explain the good agreement between G4 and M06-2X/6-311++G(d,p) for the AIE of naphthalene and the overestimation with CBS-QB3. Finally, the accuracy of M06-2X/6-311++G(d,p) is comparable to (R)CCSD(T) calculations for the AIE of naphthalene. The electronic structure based CBS extrapolation method typically involves using data from multiple levels of theory and basis sets to estimate the energy at the complete basis set limit, which is considered to be the most accurate result. In this case, if the CBS extrapolation was based on energies obtained from CCSD(T) calculations with cc-pVDZ and cc-pVTZ basis sets, there could be some limitations associated with the accuracy of these lower-level calculations. Besides, (R)CCSD(T)-F12 is a highly accurate post-SCF (self-consistent field) method that includes electron correlation effects explicitly. Table 1 shows that M06-2X/6-311++G(d,p) performs even better than this reference ab initio method. It is possible that for the AIE of naphthalene, the level of electron correlation included in M06-2X/6-311++G(d,p) is sufficient to provide accurate results, while the higher-order correlation effects captured by (R)CCSD(T)-F12/aug-cc-pVDZ may not be as crucial.

The choice of basis set can also impact the accuracy of calculated AIEs. (R)CCSD(T)-F12/aug-cc-pVDZ uses an augmented correlation-consistent basis set (in conjunction with the corresponding density

fitting and resolution of identity basis sets), while M06-2X/6-311++G(d,p) uses a DFT-specific basis set. The basis set size and quality can affect the description of electron orbitals and their energies, and can have an impact on the accuracy of calculated AIEs. Regarding the results, it seems that the basis set used in M06-2X/6-311++G(d,p) is better suited for describing the electronic structure of naphthalene in the context of AIE calculations.

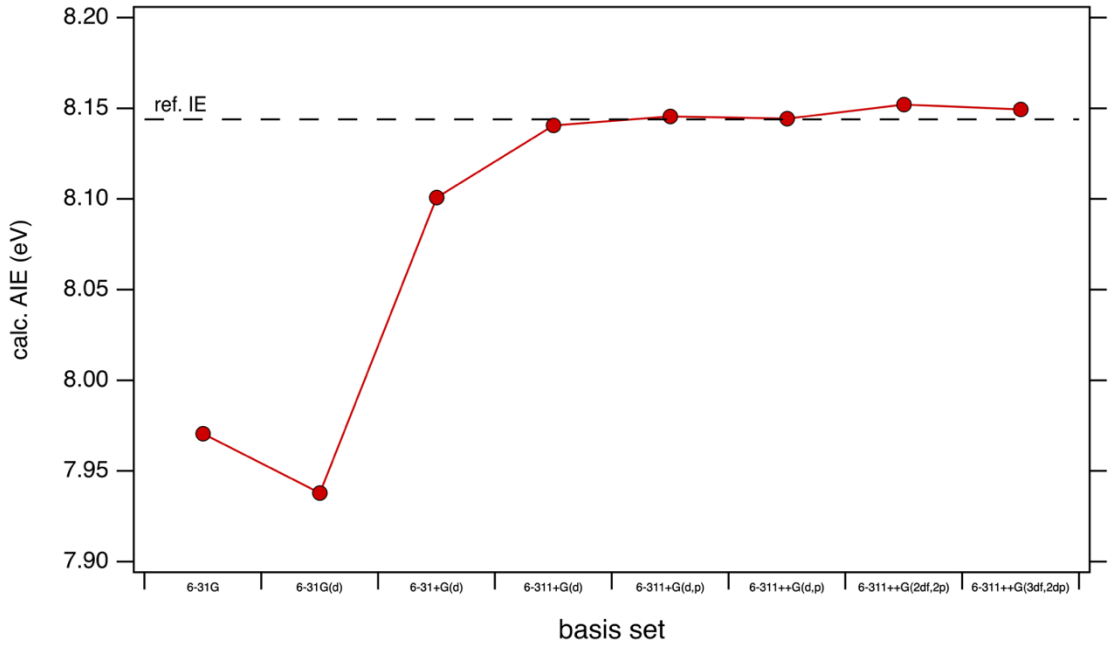

Figure 1. Calculated AIE of naphthalene using M06-2X with various Pople basis sets compared to the referenced ionization energy of naphthalene from Cockett et al.[33] (horizontal dashed line).

Basis set effects were probed to assess an appropriate level of theory for AIE calculations with the M06-2X functional and the 6-31G, 6-31G(d), 6-31+G(d), 6-311+G(d), 6-311+G(d,p), 6-311++G(d,p), 6-311++G(2df,2p), and 6-311++G(3df,2dp) basis sets. Figure 1 shows minimal changes in the AIE of naphthalene when different basis sets are used beyond M06-2X/6-311+G(d) and that the AIE is even overestimated when the basis set is increased to M06-2X/6-311++G(3df,2dp). One can think that the distribution of electron density near the ionization site may also be overestimated by basis sets with more diffuse functions. Diffuse functions are designed to capture electron density that is spread out over larger regions of space, including regions further away from the atomic nucleus. While they improve the accuracy of calculations involving long-range interactions and electron correlation, they may potentially lead to an overestimation of the AIE in certain cases. When the ionization process involves removing an electron from a localized orbital, the inclusion of diffuse functions can artificially enhance the electron density in the vicinity of the ionization site, resulting in an exaggerated stabilization effect.

176

177 **Table 2.** Chemical structures of the molecular species investigated presently.

	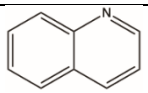	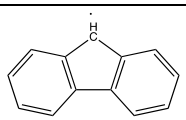	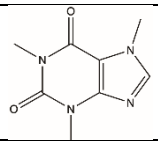	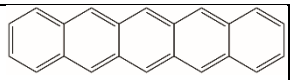
pyrrole	**quinoline**	**fluorenyl**	**caffeine**	**pentacene**
	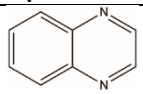	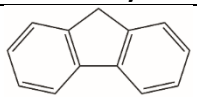	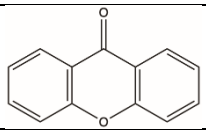	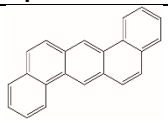
benzene	**quinoxaline**	**fluorene**	**xanthone**	**dibenz[a,h]anthracene**
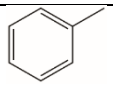	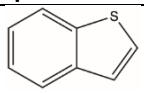	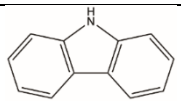	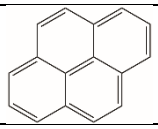	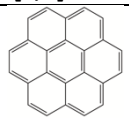
toluene	**benzo[b]thiophene**	**carbazole**	**pyrene**	**coronene**
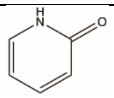	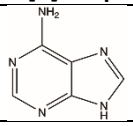	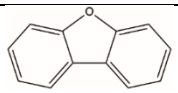	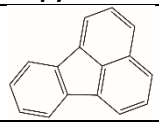	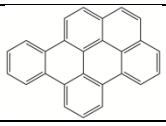
2-pyridone	**adenine**	**dibenzofuran**	**fluoranthene**	**dibenzo[b,pqr]perylene**
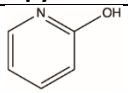	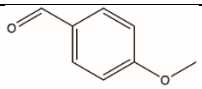	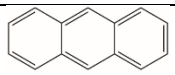	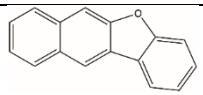	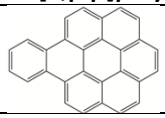
2-hydroxypyridine	**anisaldehyde**	**anthracene**	**benzo[b]naphtho[2,3-d]furan**	**benzo[a]coronene**
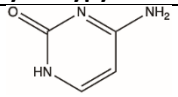	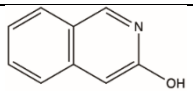	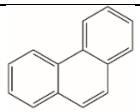	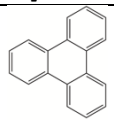	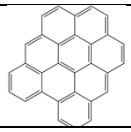
cytosine	**3-hydroxyisoquinoline**	**phenanthrene**	**triphenylene**	**dibenzo[bc,ef]coronene**
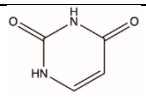	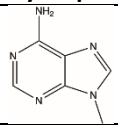	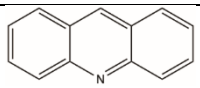	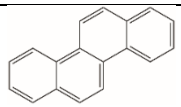	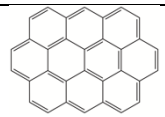
uracil	**9-methyl adenine**	**acridine**	**chrysene**	**ovalene**
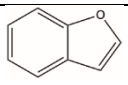	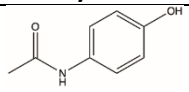	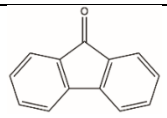	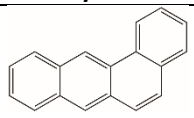	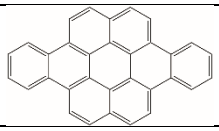
2,3-benzofuran	**paracetamol**	**fluorenone**	**benz[a]anthracene**	**dibenzo[a,j]coronene**
purine	**acenaphthylene**	**1,2-acenaphthenequinone**	**perylene**	**circumcoronene**
thymine	**acenaphthene**	**benzophenone**	**benzo[a]pyrene**	**circumcircumcoronene**

naphthalene	1-naphthaldehyde	dibenzothiophene	benzo[ghi]perylene

178

179 **Table 3.** Calculated AIEs (in eV) in this work of various PAHs and substituted analogues with M06-
180 2X/6-311+G(d), (R)CCSD(T)-F12/aug-cc-pVDZ and compared to reference experimental values from
181 the literature. The chemical structures are given in Table 2. A hyphen indicates either the failure of
182 convergence in the calculation or the absence of a reference for the AIE in the literature.

Molecular mass (u)	Name	Exp.	Calc. (M06-2X/6-311+G(d))	Calc. ((R)CCSD(T)-F12/aug-cc-pVDZ)
67	pyrrole	8.207[42]	8.211	8.166
78	benzene	9.243[42]	9.211	9.234
92	toluene	8.828[42]	8.778	8.803
95	2-pyridone	8.443[43]	8.482	8.430
	2-hydroxypyridine	8.933[43]	8.942	8.916
111	cytosine	8.738[44]	8.835	8.773
112	uracil	9.32[45]	9.39	9.337
118	2,3-benzofuran	8.35[46]	8.355	8.314
120	purine	9.12[45]	9.33	9.122
126	thymine	8.913[47]	8.931	8.909
128	naphthalene	8.144[42]	8.141	8.121
129	quinoline	8.63[42]	8.625	8.623
130	quinoxaline	8.89[48]	9.015	8.882
134	Benzo[b]thiophene	8.73[42]	8.758	-
136	anisaldehyde	8.60[42]	8.611	8.542
135	adenine	8.264[49]	8.294	8.260
145	3-hydroxyisoquinoline	8.028[50]	8.08	8.065
149	9-methyl adenine	8.097[51]	8.121	8.079
151	paracetamol	7.57	7.66	7.682
152	acenaphthylene	8.12[42]	8.006	7.985
154	acenaphthene	7.75[42]	7.695	7.682
156	1-naphthaldehyde	8.43[42]	8.452	8.396
165	Fluorenyl	7.07[52]	7.10	-
166	fluorene	7.91[42]	7.918	7.881
167	carbazole	7.57[42]	7.695	7.661
168	dibenzofuran	8.12[46]	8.175	8.095
178	anthracene	7.439[42]	7.388	7.400
	phenanthrene	7.89[42]	7.898	7.891
179	acridine	7.8[42]	7.896	7.888
180	fluorenone	8.356[53]	8.406	8.491
182	1,2-acenaphthenequinone	8.77[42]	8.867	8.776
	benzophenone	8.923[53]	8.94	-
184	dibenzothiophene	7.90[42]	7.993	-
194	caffeine	7.95[42]	8.077	7.998
196	xanthone	8.42[42]	8.508	8.440
202	pyrene	7.43[42]	7.431	7.396
	fluoranthene	7.90[42]	7.896	7.868
218	benzo[b]naphtho[2,3-	7.64[46]	7.673	7.632

	d]furan			
228	triphenylene	7.87[42]	7.892	-
	chrysene	7.60[42]	7.585	-
	Benz[a]anthracene	7.45[42]	7.391	-
252	perylene	6.96[42]	6.965	-
	Benzo[a]pyrene	7.12[42]	7.093	-
276	Benzo[ghi]perylene	7.17[42]	7.171	-
278	pentacene	6.63[42]	6.504	-
	Dibenz[a,h]anthracene	7.39[42]	7.355	-
300	coronene	7.31[54]	7.393	-
326	Dibenzo[b,pqr]perylene	7.12[42]	7.206	-
350	Benzo[a]coronene	7.08[42]	7.192	-
374	Dibenzo[bc,ef]coronene	6.50[42]	6.521	-
398	ovalene	6.86[42]	6.776	-
400	Dibenzo[a,j]coronene	6.92[42]	7.007	-
666	circumcoronene	-	6.572	-
1,176	circumcircumcoronene	-	6.082	-

To verify the suitability of the M06-2X/6-311+G(d) method for calculating the AIEs of various PAHs and their substituted analogues, a specific investigation was conducted. Initially, the validity of this method was established by successfully calculating the AIE of naphthalene. Subsequently, in order to comprehensively explore the AIEs of a wide range of aromatic molecules, 54 PAHs and substituted analogues with masses ranging from 67 atomic mass unit (u) to 1,176 u (as detailed in Table 3) were subjected to AIE calculations using the M06-2X/6-311+G(d) method. These calculated AIE values were then compared to both the corresponding experimental values published in literature and the AIE values determined using the (R)CCSD(T)-F12/aug-cc-pVDZ method, which is considered as the reference method for AIE calculations.

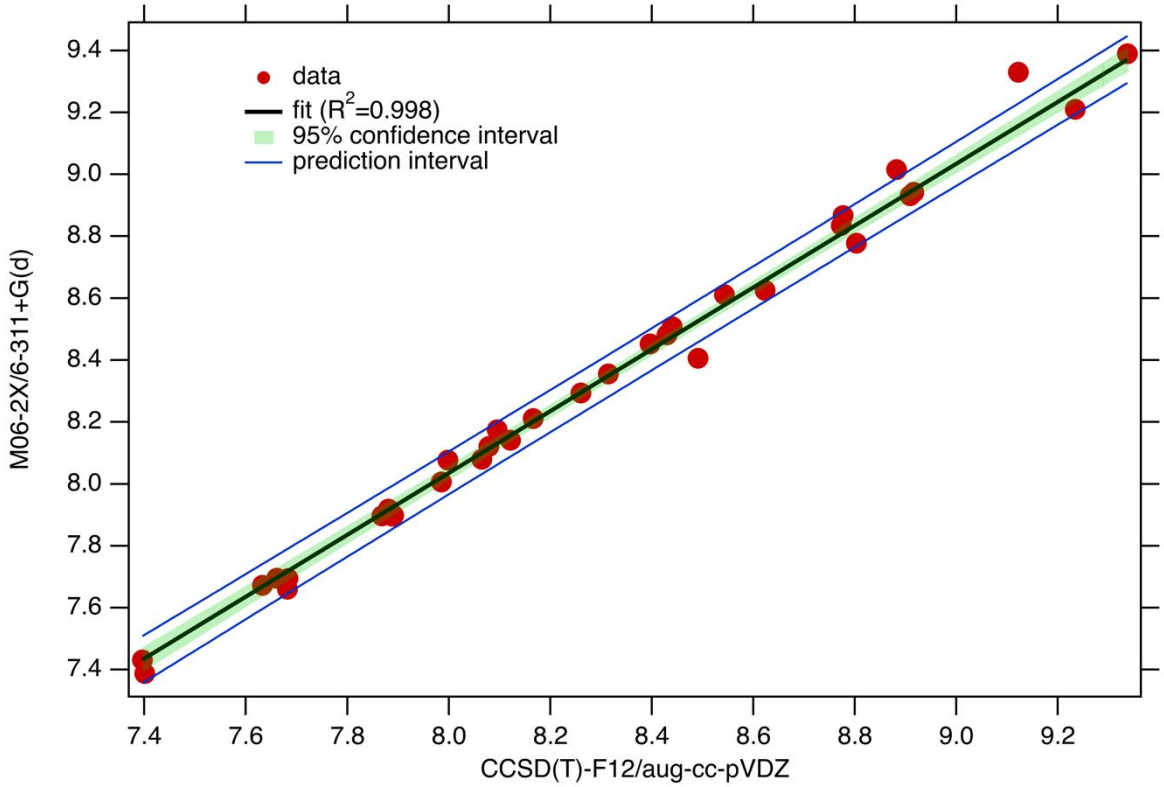

Figure 2. Plot of the calculated AIE for various PAHs and substituted analogues (as specified in Tables 2 and 3) with M06-2X/6-311+G(d) as a function of the AIE calculated with (R)CCSD(T)-F12/aug-cc-pVDZ. The black line corresponds to the linear regression of the data. The green area shows a confidence level to 95% and the blue line are prediction bands. The corresponding values are listed in Table 3.

In Figure 2, a least-squares regression analysis is presented, showcasing the relationship between the two sets of AIE values calculated using the M06-2X/6-311+G(d) and (R)CCSD(T)-F12/aug-cc-pVDZ methods. Due to computational resource limitations, (R)CCSD(T)-F12 calculations were performed for molecules with molar masses up to 218 u. The high correlation coefficient (R^2=0.998) observed in these data demonstrates a strong correlation, reinforcing the trend observed for naphthalene. This finding indicates that the M06-2X/6-311+G(d) method is consistent and sufficiently reliable for predicting the AIEs of these molecules.

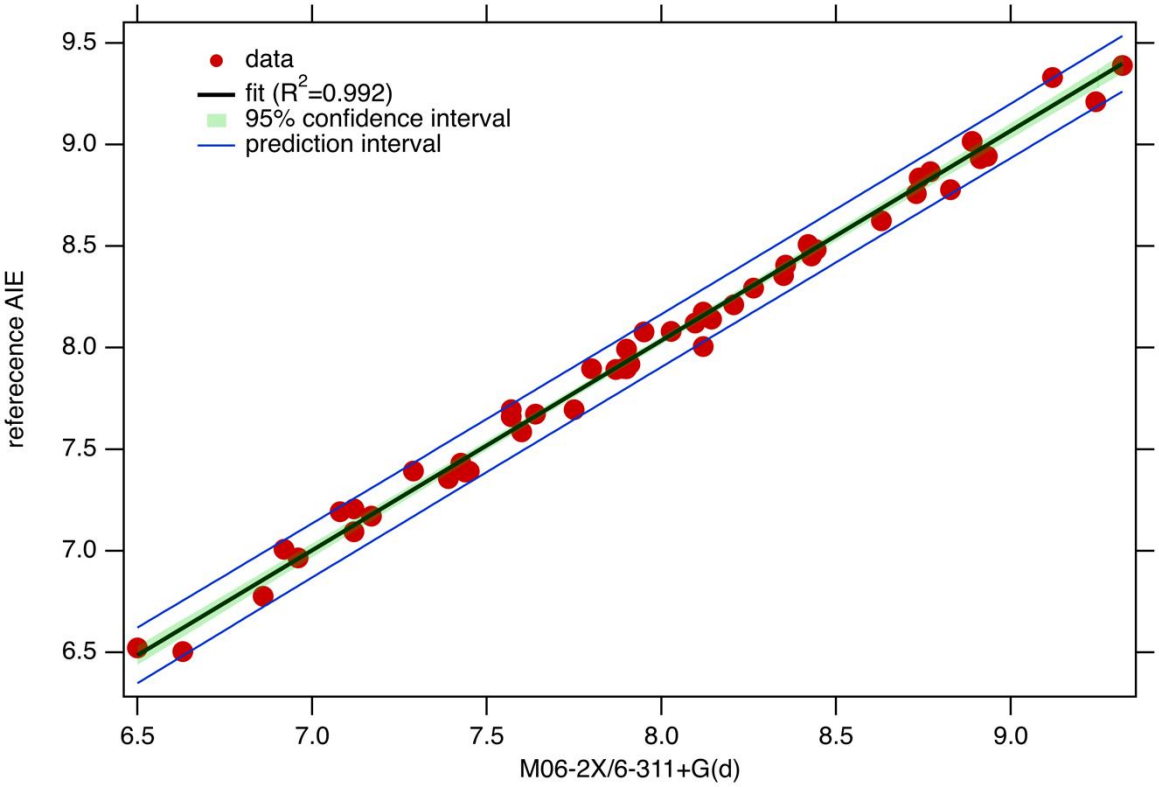

Figure 3. Comparison between calculated AIEs with M06-2X/6-311+G(d) and reference AIEs from the literature for various PAHs and substituted analogues as specified in Tables 2 and 3.

To further expand the range of tested molecules and validate the reliability of the method, the comparison between calculated AIEs using the M06-2X/6-311+G(d) method was extended to experimental values reported in the literature. This included data from high-resolution photoelectron photoion coincidence (PEPICO) spectroscopic studies (e.g., Laamiri et al.[51] and Schleier et al.[48]) as well as information available in the National Institute of Standards and Technology (NIST) database.[42] In this context, AIEs were calculated for 52 PAHs and substituted analogues, with molecular masses ranging from 67 u to 400 u, using the M06-2X/6-311+G(d) computational method as listed in Table 2. The molecular structures of these compounds consist of multiple fused benzene rings, with some containing heteroatoms such as nitrogen (N), oxygen (O), sulfur (S), and various functional groups (as detailed in Table 2). Figure 3 illustrates the least-squares regression analysis performed between the experimental AIE values and the corresponding ones calculated using M06-2X/6-311+G(d). A high correlation coefficient (R^2=0.992) is obtained, indicating a strong correlation between the predicted AIE values using M06-2X/6-311+G(d) and the reference values from the literature within the energy range of 6.5 – 9.4 eV. Once again, this result provides further support for the remarkable reliability of M06-2X/6-311+G(d) in predicting the AIEs of PAHs and substituted analogues, from relatively small molecular systems to very large structures.

Tables 2 and 3 demonstrate that the predictive accuracy of the M06-2X/6-311+G(d) approach is valuable for distinguishing between structural isomers of PAHs, such as pyrene and fluoranthene (m/z 202), which have a similar chemical formula ($C_{16}H_{10}$) but differ in molecular structure. This structural distinction impacts the chemical and reactive properties of these compounds. The application of this theoretical method in investigating the formation of such isomers in photoionization experiments is highly significant significance for gaining insights into reaction mechanisms and exploring structure-property relationships.[55]

As shown in the case of fluorenyl (m/z 165) and fluorene (m/z 166), resonance-stabilized radicals are also one of the target of interest for this method with a high accuracy/time ratio. These radicals are expected to be involved in the formation of soot particles whose formation mechanisms remain incomplete.[10] The use of this theoretical method would thus benefit the photoionization experiments used for the characterization of large persistent radicals in nascent soot as well as obtaining structural information on the aromatic units.[56]

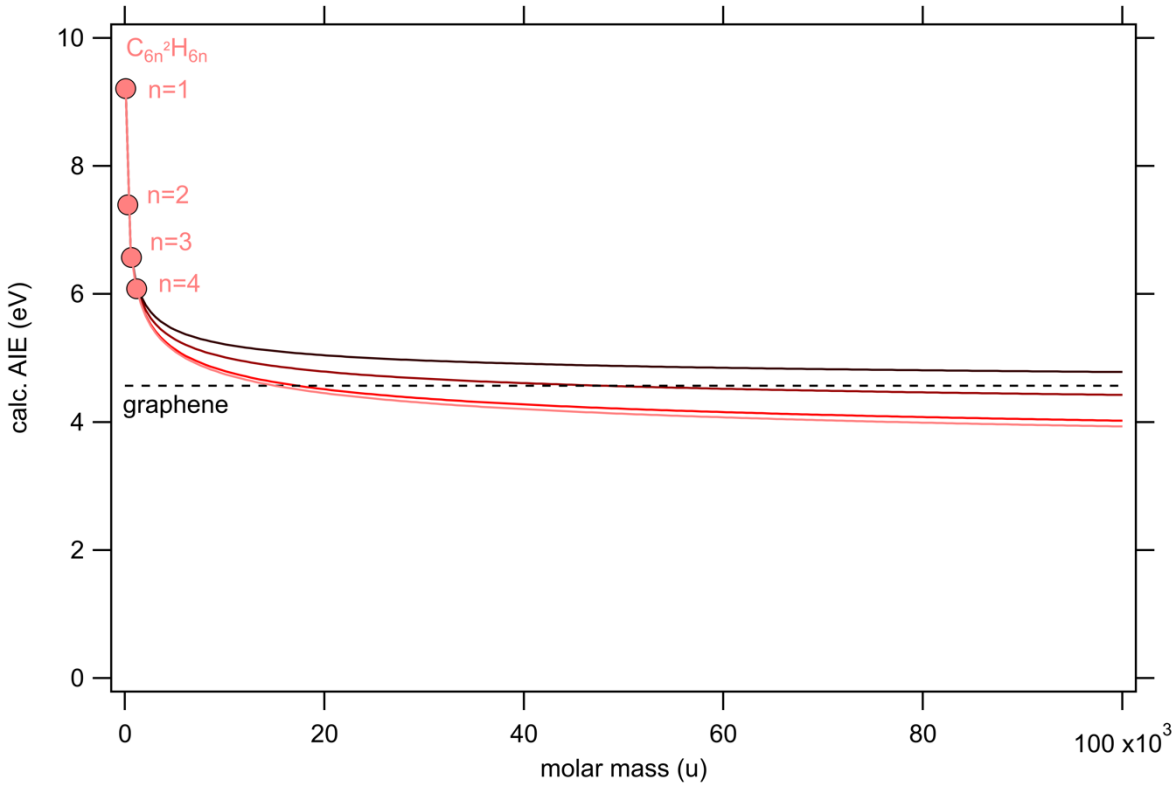

Figure 4. Comparison between the calculated AIEs of $C_{6n^2}H_{6n}$ (n = 1–4) species (red dots) using the M06-2X/6-311+G(d) method and a reference value the ionization energy of graphene (black dashed line)[57]. Different fit of the data using a power function is represented by colored solid lines. Further information can be found in the text.

In order to provide predictive insights, AIE calculations were conducted using the benchmarked M06-2X/6-311+G(d) method for larger PAH systems that lack literature values. The focus was on investigating a specific group of coronene-derivative species with a general $C_{6n^2}H_{6n}$ molecular formula. These compounds share a specific structural pattern characterized by the arrangement of six carbon atoms forming cyclic, aromatic configurations. In this work, the number of these cyclic units, denoted as *n*, was varied from 1 to 4 (C_6H_6 to $C_{96}H_{24}$), allowing for the exploration of a range of compounds from benzene to more complex structures: coronene, circumcoronene, and circumcircumcoronene. The AIEs obtained from calculations for coronene-derived species were compared to a referenced ionization potential of graphene: 4.57 ± 0.05 eV.[57] The results, shown in Figure 4, indicate that as the size of the PAHs increases, their AIEs approach the value of graphene. This implies that the electrons become less tightly bound as the molecule size expands, indicating an evolution in the electronic structure of the PAHs. This observation aligns with the expectations derived from the Hückel simple model for such aromatic compounds. The fact that the ionization energies of PAHs approach that of graphene upon extending the π-aromatic system suggests a convergence of their electronic properties from molecules to extended 2D materials. This may indicate that large-sized PAHs exhibit electronic properties close to those of graphene, which can be important for potential applications such as the development of new PAH-based materials with interesting electrical conduction properties. The graphene-like electronic properties could also be useful in the design of electronic devices or in areas such as nanochemistry, nanotechnology, catalysis and energy conversion.

The AIEs of $C_{6n^2}H_{6n}$ (n = 1–4) species were fitted and extrapolated using a power function with the form $y_0 + A\,x^B$. In this equation, the constant term (y_0) should correspond to the theoretical AIE of graphene. Figure 4 presents four fits using different values for the larger masses, resulting in significant variations in the y_0 term and on the B power in this fitting function. This discrepancy arises because the calculated AIEs data primarily fall within the repulsive region of the fit rather than the convergent flat part. Accordingly, even when considering a PAH greater than 1,000 u, the AIE values remain considerably distant from that of graphene. Consequently, these species cannot be considered as substitutes for graphene in terms of their physico-chemical properties.

Furthermore, it is important to acknowledge that the differences between the reference value of graphene and the AIE values of PAHs could also be attributed to the presence of Jahn-Teller (JT) distortions in the cationic structures of PAHs. Similar to coronene, as discussed in Tampieri et al.[58], both circumcoronene and circumcircumcoronene have highly symmetric neutral ground states with doubly degenerate HOMOs and LUMOs. When one electron is removed to form a cation, the partially filled degenerate molecular orbitals lead to an electronic instability. Consequently, this cation undergoes structural relaxation to minimize this instability. This relaxation manifests as a geometric

distortion, breaking the molecular symmetry and reducing the energy of the system. In this work, by considering the changes in bond length between the ionic and neutral forms, the relative elongation and restriction of the bond lengths are found to be consistent across different-sized PAHs but the overall extent of the changes diminishes as the molecules become larger.

To summarize this work shows that M06-2X outperforms the common DFT methods in predicting the AIEs of PAHs and substituted analogues. For those specific molecular systems, the level of accuracy of M06-2X is comparable to the highly accurate (R)CCSD(T)-F12 which is time consuming as the size of the molecular system increases. Comparison with existing AIE values from the literature shows that the M06-2X is also able to accurately predict the AIEs of large aromatic molecular systems. In this work the bigger structures whose AIE has been calculated includes 37 fused benzene rings and 96 carbon atoms. Such accuracy from M06-2X is mainly related to the large quantity of HF exchange that this DFT contains compared to other DFTs. Another important aspect might also be the Rydberg character of certain excited states of PAHs which are highly excited electronic states with diffuse electron densities.[59] M06-2X has been designed to describe diffuse wave functions which could potentially make it suitable for accurately predicting properties associated with Rydberg-like states.[60] This finding suggests that M06-2X, with the recommendation of a proper basis set, is a reliable and efficient method to be used in conjunction with experimental techniques for gaining a comprehensive understanding of the electronic properties of PAHs and related molecules. Particularly the low-lying Rydberg states, are not yet fully understood despite extensive research as the lowest members of the Rydberg series can deviate from pure Rydberg states due to the proximity to the molecular core. This results in mixing with valence states of similar energy, leading to complex electronic structures and spectroscopic features, are of considerable interest for combustion, atmospheric, molecular electronics[61] and astrochemistry[62].

The set of molecules that was used to confront the predictions of M06-2X in this work includes PAHs with hetero-atoms that can be formed from biofuels or constitute nucleic acid bases. Thus having calculated AIEs to be able to identify those species in photoionization experiments using either coincidence detection schemes and mass spectrometry could be of great interest with many applications. Accurate calculation of AIEs for PAHs and their substituted analogues is important for understanding their electronic properties, predicting their reactivity and stability, designing functional materials, and evaluating their environmental and health implications. Since nucleobases (NBs) are the building blocks of both ribonucleic (RNA) and deoxyribonucleic acid (DNA), calculating the AIE of NBs is important for understanding the stability and reactivity of RNA and DNA, predicting DNA damage, studying DNA repair mechanisms, and aiding in drug design and development targeting nucleic acids. However, it is important to note that the accuracy and reliability of any computational method, including M06-2X, depend on the specific system being studied and the desired level of

accuracy. It is always prudent to validate the results of any computational method against experimental data or higher-level calculations to ensure the accuracy of the findings.

COMPUTATIONAL METHODS

All electronic structure and energy computations were performed using GAUSSIAN09[63] and MOLPRO[64] suites of *ab initio* programs. To compute AIEs, full structure optimizations on neutral and cationic species were carried out using tight conversion criteria and by formally lowering the symmetry in the calculations (i.e. in C_1 point group). The optimized structure of the neutral species was used as the initial structure for the cationic forms. DFT and composite methods computations include full geometry optimizations and zero-point energy (ΔZPE) correction. Coupled clusters methods, (R)CCSD(T)/CBS and (R)CCSD(T)-F12/aug-cc-pVDZ, as implemented in MOLPRO, were used for single point computations on top of the optimized neutral and cationic structures as determined by M06-2X/6-311+G(d). For the respective AIEs, we also used the ΔZPE, and frequencies as calculated at the M06-2X/6-311+G(d) level of theory. Only for the biggest species calculated in this work, $C_{96}H_{24}$, the ΔZPE was derived from frequency calculations at the M06-2X/6-31G(d) level of theory after optimization. The CCSD(T)/CBS energies were extrapolated from CCSD(T)/cc-pVDZ, and CCSD(T)/cc-pVTZ energies using the scheme suggested by Martin[65] and Feller and Dixon[66].

AUTHOR INFORMATION

Corresponding authors

Jérémy Bourgalais - Université de Lorraine, CNRS, LRGP, F-54000 Nancy, France ; ORCID : 0000-0003-4710-8943 ; Email : jeremy.bourgalais@cnrs.fr

Majdi Hochlaf - Université Gustave Eiffel, COSYS/IMSE, 77454 Champs sur Marne, France ; ORCID : 0000-0002-4737-7978 ; Email : majdi.hochlaf@univ-eiffel.fr

AUTHORS

Xavier Mercier

Université de Lille, CNRS, PC2A, F-59000, Lille, France. Email: xavier.mercier@univ-lille.fr

Muneerah Mogren Al-Mogren

Department of Chemistry, College of Sciences, King Saud University, PO Box 2455, Riyadh 11451, Saudi Arabia. Email: mmogren@ksu.edu.sa

ACKNOWLEDGEMENTS

This work was performed using HPC resources from GENCI-IDRIS (Grant 2023-AD010814091) and the EXPLOR centre hosted by the University of Lorraine (Project: 2021EXTXX2356). The authors extend

their appreciation to the Researchers supporting project number (RSPD2023R808) King Saud University, Riyadh, Saudi Arabia. The authors thank Prof. C. Adamo (France) for engaging in fruitful discussions.

REFERENCES

(1) Idowu, O.; Semple, K. T.; Ramadass, K.; O'Connor, W.; Hansbro, P.; Thavamani, P. Beyond the Obvious: Environmental Health Implications of Polar Polycyclic Aromatic Hydrocarbons. *Environment International* **2019**, *123*, 543–557. https://doi.org/10.1016/j.envint.2018.12.051.

(2) Sampaio, G. R.; Guizellini, G. M.; da Silva, S. A.; de Almeida, A. P.; Pinaffi-Langley, A. C. C.; Rogero, M. M.; de Camargo, A. C.; Torres, E. A. F. S. Polycyclic Aromatic Hydrocarbons in Foods: Biological Effects, Legislation, Occurrence, Analytical Methods, and Strategies to Reduce Their Formation. *International Journal of Molecular Sciences* **2021**, *22* (11), 6010. https://doi.org/10.3390/ijms22116010.

(3) Premnath, N.; Mohanrasu, K.; Guru Raj Rao, R.; Dinesh, G. H.; Prakash, G. S.; Ananthi, V.; Ponnuchamy, K.; Muthusamy, G.; Arun, A. A Crucial Review on Polycyclic Aromatic Hydrocarbons - Environmental Occurrence and Strategies for Microbial Degradation. *Chemosphere* **2021**, *280*, 130608. https://doi.org/10.1016/j.chemosphere.2021.130608.

(4) Keyte, I. J.; Harrison, R. M.; Lammel, G. Chemical Reactivity and Long-Range Transport Potential of Polycyclic Aromatic Hydrocarbons–a Review. *Chemical Society Reviews* **2013**, *42* (24), 9333–9391.

(5) Kim, K.-H.; Jahan, S. A.; Kabir, E.; Brown, R. J. A Review of Airborne Polycyclic Aromatic Hydrocarbons (PAHs) and Their Human Health Effects. *Environment international* **2013**, *60*, 71–80.

(6) Parker, D. S. N.; Kaiser, R. I. On the Formation of Nitrogen-Substituted Polycyclic Aromatic Hydrocarbons (NPAHs) in Circumstellar and Interstellar Environments. *Chem. Soc. Rev.* **2017**, *46* (2), 452–463. https://doi.org/10.1039/C6CS00714G.

(7) Kaiser, R. I.; Parker, D. S.; Mebel, A. M. Reaction Dynamics in Astrochemistry: Low-Temperature Pathways to Polycyclic Aromatic Hydrocarbons in the Interstellar Medium. *Annual Review of Physical Chemistry* **2015**, *66*, 43–67.

(8) Joblin, C.; Tielens, A. G. G. M. *PAHs and the Universe*; EDP Sciences, 2021.

(9) Richter, H.; Howard, J. B. Formation of Polycyclic Aromatic Hydrocarbons and Their Growth to Soot—a Review of Chemical Reaction Pathways. *Progress in Energy and Combustion science* **2000**, *26* (4–6), 565–608.

(10) Johansson, K. O.; Head-Gordon, M. P.; Schrader, P. E.; Wilson, K. R.; Michelsen, H. A. Resonance-Stabilized Hydrocarbon-Radical Chain Reactions May Explain Soot Inception and Growth. *Science* **2018**, *361* (6406), 997–1000. https://doi.org/10.1126/science.aat3417.

(11) Homann, K.-H. Fullerenes and Soot Formation—New Pathways to Large Particles in Flames. *Angewandte Chemie International Edition* **1998**, *37* (18), 2434–2451.

(12) Wang, H. Formation of Nascent Soot and Other Condensed-Phase Materials in Flames. *Proceedings of the Combustion institute* **2011**, *33* (1), 41–67.

(13) Frenklach, M. Reaction Mechanism of Soot Formation in Flames. *Physical chemistry chemical Physics* **2002**, *4* (11), 2028–2037.

(14) Anthony, J. E. Functionalized Acenes and Heteroacenes for Organic Electronics. *Chemical reviews* **2006**, *106* (12), 5028–5048.

(15) Anthony, J. E. The Larger Acenes: Versatile Organic Semiconductors. *Angewandte Chemie International Edition* **2008**, *47* (3), 452–483.

(16) Fischer, I.; Pratt, S. T. Photoelectron Spectroscopy in Molecular Physical Chemistry. *Phys. Chem. Chem. Phys.* **2022**, *24* (4), 1944–1959. https://doi.org/10.1039/D1CP04984D.

(17) Hemberger, P.; Bodi, A.; Bierkandt, T.; Köhler, M.; Kaczmarek, D.; Kasper, T. Photoelectron Photoion Coincidence Spectroscopy Provides Mechanistic Insights in Fuel Synthesis and Conversion. *Energy Fuels* **2021**, *35* (20), 16265–16302. https://doi.org/10.1021/acs.energyfuels.1c01712.

(18) Baer, T.; P. Tuckett, R. Advances in Threshold Photoelectron Spectroscopy (TPES) and Threshold Photoelectron Photoion Coincidence (TPEPICO). *Physical Chemistry Chemical Physics* **2017**, *19* (15), 9698–9723. https://doi.org/10.1039/C7CP00144D.
(19) Hochlaf, M. Advances in Spectroscopy and Dynamics of Small and Medium Sized Molecules and Clusters. *Physical Chemistry Chemical Physics* **2017**, *19* (32), 21236–21261. https://doi.org/10.1039/C7CP01980G.
(20) Dyke, J. M. Photoionization Studies of Reactive Intermediates Using Synchrotron Radiation. *Phys. Chem. Chem. Phys.* **2019**, *21* (18), 9106–9136. https://doi.org/10.1039/C9CP00623K.
(21) Mercier, X.; Faccinetto, A.; Batut, S.; Vanhove, G.; Božanić, D. K.; Hróðmarsson, H. R.; Garcia, G. A.; Nahon, L. Selective Identification of Cyclopentaring-Fused PAHs and Side-Substituted PAHs in a Low Pressure Premixed Sooting Flame by Photoelectron Photoion Coincidence Spectroscopy. *Phys. Chem. Chem. Phys.* **2020**, *22* (28), 15926–15944. https://doi.org/10.1039/D0CP02740E.
(22) Purvis III, G. D.; Bartlett, R. J. A Full Coupled-Cluster Singles and Doubles Model: The Inclusion of Disconnected Triples. *The Journal of Chemical Physics* **1982**, *76* (4), 1910–1918.
(23) Raghavachari, K.; Trucks, G. W.; Pople, J. A.; Head-Gordon, M. A Fifth-Order Perturbation Comparison of Electron Correlation Theories. *Chemical Physics Letters* **1989**, *157* (6), 479–483.
(24) Cohen, A. J.; Mori-Sánchez, P.; Yang, W. Challenges for Density Functional Theory. *Chemical reviews* **2012**, *112* (1), 289–320.
(25) Friesner, R. A. Ab Initio Quantum Chemistry: Methodology and Applications. *Proceedings of the National Academy of Sciences* **2005**, *102* (19), 6648–6653.
(26) Hammes-Schiffer, S. A Conundrum for Density Functional Theory. *Science* **2017**, *355* (6320), 28–29.
(27) Semmeq, A.; Ouaskit, S.; Monari, A.; Badawi, M. Ionization and Fragmentation of Uracil upon Microhydration. *Phys. Chem. Chem. Phys.* **2019**, *21* (9), 4810–4821. https://doi.org/10.1039/C8CP07452F.
(28) Zhao, Y.; Truhlar, D. G. The M06 Suite of Density Functionals for Main Group Thermochemistry, Thermochemical Kinetics, Noncovalent Interactions, Excited States, and Transition Elements: Two New Functionals and Systematic Testing of Four M06-Class Functionals and 12 Other Functionals. *Theor Chem Account* **2008**, *120* (1), 215–241. https://doi.org/10.1007/s00214-007-0310-x.
(29) Mardirossian, N.; Head-Gordon, M. How Accurate Are the Minnesota Density Functionals for Noncovalent Interactions, Isomerization Energies, Thermochemistry, and Barrier Heights Involving Molecules Composed of Main-Group Elements? *J. Chem. Theory Comput.* **2016**, *12* (9), 4303–4325. https://doi.org/10.1021/acs.jctc.6b00637.
(30) Goerigk, L.; Hansen, A.; Bauer, C.; Ehrlich, S.; Najibi, A.; Grimme, S. A Look at the Density Functional Theory Zoo with the Advanced GMTKN55 Database for General Main Group Thermochemistry, Kinetics and Noncovalent Interactions. *Physical Chemistry Chemical Physics* **2017**, *19* (48), 32184–32215.
(31) Zhang, J.; Valeev, E. F. Prediction of Reaction Barriers and Thermochemical Properties with Explicitly Correlated Coupled-Cluster Methods: A Basis Set Assessment. *Journal of chemical theory and computation* **2012**, *8* (9), 3175–3186.
(32) Tew, D. P. Principal Domains in F12 Explicitly Correlated Theory. In *Advances in Quantum Chemistry*; Elsevier, 2021; Vol. 83, pp 83–106.
(33) Cockett, M. C.; Ozeki, H.; Okuyama, K.; Kimura, K. Vibronic Coupling in the Ground Cationic State of Naphthalene: A Laser Threshold Photoelectron [Zero Kinetic Energy (ZEKE)-Photoelectron] Spectroscopic Study. *The Journal of chemical physics* **1993**,

98 (10), 7763–7772.
(34) Ditchfield, R.; Hehre, W. J.; Pople, J. A. Self- Consistent Molecular- Orbital Methods. IX. An Extended Gaussian- Type Basis for Molecular- Orbital Studies of Organic Molecules. *J. Chem. Phys.* **1971**, *54* (2), 724–728. https://doi.org/10.1063/1.1674902.
(35) Becke, A. D. A New Mixing of Hartree–Fock and Local Density-Functional Theories. *The Journal of chemical physics* **1993**, *98* (2), 1372–1377.
(36) Stephens, P. J.; Devlin, F. J.; Chabalowski, C. F.; Frisch, M. J. Ab Initio Calculation of Vibrational Absorption and Circular Dichroism Spectra Using Density Functional Force Fields. *The Journal of physical chemistry* **1994**, *98* (45), 11623–11627.
(37) Adamo, C.; Barone, V. Toward Reliable Density Functional Methods without Adjustable Parameters: The PBE0 Model. *J. Chem. Phys.* **1999**, *110* (13), 6158–6170. https://doi.org/10.1063/1.478522.
(38) Chai, J.-D.; Head-Gordon, M. Systematic Optimization of Long-Range Corrected Hybrid Density Functionals. *The Journal of Chemical Physics* **2008**, *128* (8), 084106. https://doi.org/10.1063/1.2834918.
(39) Curtiss, L. A.; Redfern, P. C.; Raghavachari, K. Gaussian-4 Theory. *J. Chem. Phys.* **2007**, *126* (8), 084108. https://doi.org/10.1063/1.2436888.
(40) Montgomery, J. A.; Frisch, M. J.; Ochterski, J. W.; Petersson, G. A. A Complete Basis Set Model Chemistry. VI. Use of Density Functional Geometries and Frequencies. *J. Chem. Phys.* **1999**, *110* (6), 2822–2827. https://doi.org/10.1063/1.477924.
(41) Montgomery, J. A.; Frisch, M. J.; Ochterski, J. W.; Petersson, G. A. A Complete Basis Set Model Chemistry. VII. Use of the Minimum Population Localization Method. *J. Chem. Phys.* **2000**, *112* (15), 6532–6542. https://doi.org/10.1063/1.481224.
(42) Linstrom, P. J.; Mallard, W. G.; Eds. *NIST Chemistry WebBook, NIST Standard Reference Database Number 69*. National Institute of Standards and Technology, Gaithersburg MD, 20899 (accessed 2023-01-10).
(43) Poully, J. C.; Schermann, J. P.; Nieuwjaer, N.; Lecomte, F.; Grégoire, G.; Desfrançois, C.; Garcia, G. A.; Nahon, L.; Nandi, D.; Poisson, L.; Hochlaf, M. Photoionization of 2-Pyridone and 2-Hydroxypyridine. *Phys. Chem. Chem. Phys.* **2010**, *12* (14), 3566. https://doi.org/10.1039/b923630a.
(44) chen, Z.; Lau, K.-C.; Garcia, G. A.; Nahon, L.; Bozanic, D. K.; Poisson, L.; Al-Mogren, M. M.; Schwell, M.; Francisco, J. S.; Bellili, A.; Hochlaf, M. Identifying Cytosine-Specific Isomers via High-Accuracy Single Photon Ionization | Journal of the American Chemical Society. *Journal of the American Chemical Society* **2016**, *138* (51), 16596–16599. https://doi.org/10.1021/jacs.6b10413.
(45) Orlov, V. M.; Smirnov, A. N.; Varshavsky, Y. M. Ionization Potentials and Electron-Donor Ability of Nucleic Acid Bases and Their Analogues. *Tetrahedron Letters* **1976**, *48*, 4377.
(46) Mayer, P. M.; Bodi, A. VUV Photoprocessing of Oxygen-Containing Polycyclic Aromatic Hydrocarbons: Threshold Photoelectron Spectra. *Journal of Molecular Spectroscopy* **2021**, *377*, 111446. https://doi.org/10.1016/j.jms.2021.111446.
(47) Majdi, Y.; Hochlaf, M.; Pan, Y.; Lau, K.-C.; Poisson, L.; Garcia, G. A.; Nahon, L.; Al-Mogren, M. M.; Schwell, M. Theoretical and Experimental Photoelectron Spectroscopy Characterization of the Ground State of Thymine Cation. *J. Phys. Chem. A* **2015**, *119* (23), 5951–5958. https://doi.org/10.1021/jp510716c.
(48) Schleier, D.; Hemberger, P.; Bodi, A.; Bouwman, J. Threshold Photoelectron Spectroscopy of Quinoxaline, Quinazoline, and Cinnoline. *J. Phys. Chem. A* **2022**, *126* (14), 2211–2221. https://doi.org/10.1021/acs.jpca.2c01073.
(49) Zhao, H. Y.; Lau, K.-C.; Garcia, G. A.; Nahon, L.; Carniato, S.; Poisson, L.; Schwell, M.; Al-Mogren, M. M.; Hochlaf, M. Unveiling the Complex Vibronic Structure of the

509 Canonical Adenine Cation. *Physical Chemistry Chemical Physics* **2018**, *20* (32), 20756–
510 20765.
511 (50) Pan, Y.; Lau, K.-C.; Poisson, L.; Garcia, G. A.; Nahon, L.; Hochlaf, M. Slow
512 Photoelectron Spectroscopy of 3-Hydroxyisoquinoline. *The Journal of Physical Chemistry A*
513 **2013**, *117*, 8095–8102. https://doi.org/10.1021/jp311615u.
514 (51) Laamiri, K.; A. Garcia, G.; Nahon, L.; Houria, A. B.; Feifel, R.; Hochlaf, M.
515 Threshold Photoelectron Spectroscopy of 9-Methyladenine: Theory and Experiment. *Physical*
516 *Chemistry Chemical Physics* **2022**, *24*, 3523–3531. https://doi.org/10.1039/D1CP03729C.
517 (52) Lang, M.; Holzmeier, F.; Fischer, I.; Hemberger, P. Threshold Photoionization of
518 Fluorenyl, Benzhydryl, Diphenylmethylene, and Their Dimers. *J. Phys. Chem. A* **2013**, *117*
519 (25), 5260–5268. https://doi.org/10.1021/jp403158z.
520 (53) Gouid, Z.; Röder, A.; Miranda, B. K. C. de; Gaveau, M.-A.; Briant, M.; Soep, B.;
521 Mestdagh, J.-M.; Hochlaf, M.; Poisson, L. Energetics and Ionization Dynamics of Two
522 Diarylketone Molecules: Benzophenone and Fluorenone. *Physical Chemistry Chemical*
523 *Physics* **2019**, *21* (26), 14453–14464. https://doi.org/10.1039/C9CP02385B.
524 (54) Clar, E.; Schmidt, W. Correlations between Photoelectron and Ultraviolet Absorption
525 Spectra of Polycyclic Hydrocarbons. The Perylene, Coronene and Bisanthene Series.
526 *Tetrahedron* **1977**, *33* (16), 2093–2097.
527 (55) Sinha, S.; Rahman, R. K.; Raj, A. On the Role of Resonantly Stabilized Radicals in
528 Polycyclic Aromatic Hydrocarbon (PAH) Formation: Pyrene and Fluoranthene Formation
529 from Benzyl–Indenyl Addition. *Phys. Chem. Chem. Phys.* **2017**, *19* (29), 19262–19278.
530 https://doi.org/10.1039/C7CP02539D.
531 (56) Faccinetto, A.; Irimiea, C.; Minutolo, P.; Commodo, M.; D'Anna, A.; Nuns, N.;
532 Carpentier, Y.; Pirim, C.; Desgroux, P.; Focsa, C.; Mercier, X. Evidence on the Formation of
533 Dimers of Polycyclic Aromatic Hydrocarbons in a Laminar Diffusion Flame. *Commun Chem*
534 **2020**, *3* (1), 112. https://doi.org/10.1038/s42004-020-00357-2.
535 (57) Yu, Y.-J.; Zhao, Y.; Ryu, S.; Brus, L. E.; Kim, K. S.; Kim, P. Tuning the Graphene
536 Work Function by Electric Field Effect. *Nano Lett.* **2009**, *9* (10), 3430–3434.
537 https://doi.org/10.1021/nl901572a.
538 (58) Tampieri, F.; Barbon, A.; Tommasini, M. Analysis of the Jahn-Teller Effect in
539 Coronene and Corannulene Ions and Its Effect in EPR Spectroscopy. *Chemical Physics*
540 *Impact* **2021**, *2*, 100012. https://doi.org/10.1016/j.chphi.2021.100012.
541 (59) Robin, M. B. *Higher Excited States of Polyatomic Molecules*; Academic Press: New
542 York, 1974.
543 (60) Jacquemin, D.; Perpete, E. A.; Ciofini, I.; Adamo, C.; Valero, R.; Zhao, Y.; Truhlar,
544 D. G. On the Performances of the M06 Family of Density Functionals for Electronic
545 Excitation Energies. *Journal of Chemical Theory and Computation* **2010**, *6* (7), 2071–2085.
546 (61) Feng, X.; Pisula, W.; Müllen, K. Large Polycyclic Aromatic Hydrocarbons: Synthesis
547 and Discotic Organization. *Pure and Applied Chemistry* **2009**, *81* (12), 2203–2224.
548 https://doi.org/10.1351/PAC-CON-09-07-07.
549 (62) Tielens, A. G. G. M. Interstellar Polycyclic Aromatic Hydrocarbon Molecules. *Annu.*
550 *Rev. Astron. Astrophys.* **2008**, *46* (1), 289–337.
551 https://doi.org/10.1146/annurev.astro.46.060407.145211.
552 (63) Frisch, M. J.; Trucks, G. W.; Schlegel, H. B.; Scuseria, G. E.; Robb, M. A.;
553 Cheeseman, J. R.; Scalmani, G.; Barone, V.; Petersson, G. A.; Nakatsuji, H.; Li, X.; Caricato,
554 M.; Marenich, A. V.; Bloino, J.; Janesko, B. G.; Gomperts, R.; Mennucci, B.; Hratchian, H.
555 P.; Ortiz, J. V.; Izmaylov, A. F.; Sonnenberg, J. L.; Williams; Ding, F.; Lipparini, F.; Egidi,
556 F.; Goings, J.; Peng, B.; Petrone, A.; Henderson, T.; Ranasinghe, D.; Zakrzewski, V. G.; Gao,
557 J.; Rega, N.; Zheng, G.; Liang, W.; Hada, M.; Ehara, M.; Toyota, K.; Fukuda, R.; Hasegawa,
558 J.; Ishida, M.; Nakajima, T.; Honda, Y.; Kitao, O.; Nakai, H.; Vreven, T.; Throssell, K.;

559 Montgomery Jr., J. A.; Peralta, J. E.; Ogliaro, F.; Bearpark, M. J.; Heyd, J. J.; Brothers, E. N.;
560 Kudin, K. N.; Staroverov, V. N.; Keith, T. A.; Kobayashi, R.; Normand, J.; Raghavachari, K.;
561 Rendell, A. P.; Burant, J. C.; Iyengar, S. S.; Tomasi, J.; Cossi, M.; Millam, J. M.; Klene, M.;
562 Adamo, C.; Cammi, R.; Ochterski, J. W.; Martin, R. L.; Morokuma, K.; Farkas, O.;
563 Foresman, J. B.; Fox, D. J. Gaussian 09 Rev. D.01, 2013.
564 (64) Werner, H.-J.; Knowles, P. J.; Knizia, G.; Manby, F. R.; Schütz, M. Molpro: A
565 General-Purpose Quantum Chemistry Program Package. *WIREs Computational Molecular*
566 *Science* **2012**, *2* (2), 242–253. https://doi.org/10.1002/wcms.82.
567 (65) Martin, J. M. L. Ab Initio Total Atomization Energies of Small Molecules — towards
568 the Basis Set Limit. *Chemical Physics Letters* **1996**, *259* (5–6), 669–678.
569 https://doi.org/10.1016/0009-2614(96)00898-6.
570 (66) Feller, D.; Dixon, D. A. Extended Benchmark Studies of Coupled Cluster Theory
571 through Triple Excitations. *The Journal of Chemical Physics* **2001**, *115* (8), 3484–3496.
572 https://doi.org/10.1063/1.1388045.
573